ELSEVIER

Journal of Hazardous Materials B139 (2007) 529–536

Journal of Hazardous Materials

www.elsevier.com/locate/jhazmat

Long-term reactive transport modelling of stabilized/solidified waste: from dynamic leaching tests to disposal scenarios

Laurent De Windt [a,*], Rabia Badreddine [b], Vincent Lagneau [a]

[a] *Ecole des Mines de Paris, CG-Hydrodynamics and Reaction Group, 35 R. St-Honoré, 77300 Fontainebleau, France*

[b] *INERIS, Direction des Risques Chroniques, Unité Déchets et Sites Pollués, Parc Technologique Alata BP 2, 60550 Verneuil-en-Halatte, France*

Available online 29 March 2006

Abstract

Environmental impact assessment of hazardous waste disposal relies, among others, on standardized leaching tests characterized by a strong coupling between diffusion and chemical processes. In that respect, this study shows that reactive transport modelling is a useful tool to extrapolate laboratory results to site conditions characterized by lower solution/solid (L/S) ratios, site specific geometry, infiltration, etc. A cement solidified/stabilized (S/S) waste containing lead is investigated as a typical example. The reactive transport model developed in a previous study to simulate the initial state of the waste as well as laboratory batch and dynamic tests is first summarized. Using the same numerical code (HYTEC), this model is then integrated to a simplified waste disposal scenario assuming a defective cover and rain water infiltration. The coupled evolution of the S/S waste chemistry and the pollutant plume migration are modelled assessing the importance of the cracking state of the monolithic waste. The studied configurations correspond to an undamaged and fully sealed system, a few main fractures between undamaged monoliths and, finally, a dense crack-network in the monoliths. The model considers the potential effects of cracking, first the increase of rain water and carbon dioxide infiltration and, secondly, the increase of L/S ratio and reactive surfaces, using either explicit fracture representation or dual porosity approaches.

Keywords: Crack; Landfill; Leaching test; Reactive transport; Stabilized/solidified waste

1. Introduction

The reduction of the inorganic wastes impact on the environment (soil, superficial and subsoil water) and their best management require the evaluation of their short and long-term behaviours in disposal and recycling scenarios. Two types of leaching tests are usually used in such a purpose. Waste characterization tests are static experiments, performed on short duration, useful for determining the intrinsic properties of the waste with respect to one or several controlled parameters. Dynamic leaching tests run on relatively long durations and aim at estimating the long-term evolution of the waste. Coupling between diffusion, dissolution, and sometimes sorption, processes is often encountered in dynamic leaching, typically with stabilized/solidified (S/S) waste [1]. Extrapolation of laboratory results to site conditions – with lower solution/solid ratios, site specific geometry, cyclic infiltration, etc. is therefore not a straightforward task.

In that context, geochemical and reactive transport modelling can be a useful tool to bridge the gap between the short-term, small-scale laboratory experiments and the long-term, large-scale site conditions [2,3]. Reactive transport modelling has two main aspects [4]: modelling of hydrodynamic processes under saturated and unsaturated conditions, inducing mass-transfer and dispersion of chemical species (transport), and modelling of geochemical processes between water, solutes, solids and gas (reactivity). Both aspects are present simultaneously and continuously, and they are interdependent. Geochemical reactions depend on the mobility of the reactants and the residence time. Conversely, the transport depends on the chemical source-term and hydrodynamic properties of the medium may change as minerals precipitate or dissolve. Practically, that duality also means that the same code can be used for gradually simulating batch tests, dynamic tests and site conditions.

A S/S waste with a hydraulic cement binder containing lead had been chosen to illustrate the methodology, progressing from leaching tests and physical characterization of the waste to source-term and disposal simulations. The second section of the paper introduces the reactive transport model, developed in a companion paper [5], to simulate the initial state of the waste as

* Corresponding author. Fax: +33 3 01 64 69 47 03.
E-mail address: laurent.dewindt@ensmp.fr (L. De Windt).

0304-3894/$ – see front matter © 2006 Elsevier B.V. All rights reserved.
doi:10.1016/j.jhazmat.2006.03.045

well as laboratory batch and dynamic tests. In the third section, this model is then integrated to an hazardous waste simulation using the same numerical code (HYTEC). A pessimistic scenario is considered by assuming a defective cover and rain water infiltration. The coupled chemical evolution of S/S waste in the disposal and fate of the pollutant plume in the leachate collector are modelled assessing the importance of the cracking state of the monolithic waste. The reason for supporting such an investigation of crack effects is two-fold. On one hand, the assumption of fracture and cracking occurrence have some physical reliability under disposal conditions. Ageing and temperature stress may disturb joint sealing between monolithic blocks but also destabilize poorly crystallized cement phases to eventually induce a network of connected cracks in the cement-based matrix [6,7]. On the other hand, the comparison of different cracking states is a relevant application of reactive transport model since cracks and fractures both increase rain water and carbon dioxide infiltration as well as L/S ratio and reactive surfaces of waste materials.

2. Reactive transport code and thermodynamic data

2.1. Reactive transport code

All the calculations were done with the reactive transport code HYTEC [8]. This numerical code simulates advective and diffusive transport of solutes and chemical reactions (aqueous chemistry, dissolution/precipitation and sorption) at equilibrium or with kinetic control. Transport is coupled to chemistry according to the following equation:

$$\frac{\partial \omega c_i}{\partial t} = \nabla \cdot (Dd \nabla c_i - c_i U) - \frac{\partial \omega \bar{c}_i}{\partial t}$$

where the dispersive/diffusive coefficient, $Dd = De + \alpha U$. The term De is the effective diffusion coefficient, α the dispersivity, U the Darcy velocity, ω is the porosity, c_i and $\bar{c}_i$ are the mobile and immobile concentrations of a element per unit volume of solution respectively. The fixed or solid fraction is evaluated by the chemical calculations, whereas the aqueous fraction is a function of the transport processes only. From a numerical point of view, chemistry and transport are coupled through a sequential iterative algorithm. Chemistry is solved by the basis component method according to an improved Newton–Raphson algorithm. The flow and transport module is based on the representative elementary volume (REV) approach with finite volume calculation.

HYTEC is commonly used for transport in porous media under saturated and unsaturated conditions. This standard configuration was used for undamaged waste monoliths (dynamic leach test in Section 3.3 and test-case A in Section 4.1). However, fracture flow can also be taken into account by HYTEC using an explicit fracture representation or a dual porosity approach. The former approach is applicable for main fractures which can be introduced in the calculation grid explicitly. This method was used for test-case B (see Section 4.1), considering a few main fracture crossing the disposal. When the fracture density becomes too high as to be represented by grid nodes, such as in test-case C, dual porosity is an interesting option allowing for introducing fracture flow effect in a REV formalism. In its simplest form, the fractured zones are formally represented by square block-matrix of side L, where diffusion only occurs, and an implicit network of fracture subjected to an average advective flow. Omitting the chemical source-term, $\partial \omega \bar{c}_i / \partial t$, the transport equation is split up into a fracture component, *f*, and a block-matrix component, *m*:

$$\frac{\partial \omega^f c^f}{\partial t} = \nabla \cdot (Dd^f \nabla c^f - c^f U^f) + \frac{8 De^m}{L^2}(c^f - c^m)$$

$$\frac{\partial \omega^m c^m}{\partial t} = -\frac{8 De^m}{L^2}(c^f - c^m).$$

2.2. Thermodynamic data

Chemical reactions were calculated assuming local thermodynamic equilibrium. The B-dot activity model was used for ionic strength correction. The MINTEQ thermodynamic database [9] was selected for the study and enriched with additional data for cement phases such as calcium silicate hydrate (CSH) of different Ca/Si ratio (CSH 1.7, CSH 1.1 and CSH 0.8), ettringite and Friedel's salt (see Table 1). The formation of $Pb(OH)_2$ as a pure hydroxide, which is present in both the MINTEQ and HATCHES [10] databases, should be considered as a simplified formulation of more complex hydrous phases. A fitting procedure of the ANC results (Section 3.1) led to a formation constant (log K) equal to −11, close to the HATCHES value (log K = −11.9).

3. Modelling of the long-term leaching tests

3.1. Material and experiments

The porous reference material was obtained by solidification (1% PbO by weight) with a proportion of 3/4 siliceous sand and 1/4 Portland cement CEM-I, a common industrial process for hazardous waste stabilization. The water/cement ratio was 0.6. These components were cold mixed and cured at room temperature during 28 days. Calcium silicate hydrates (CSH), portlandite and sulfo-aluminates constitute the main cement solid phases. The S/S waste was cut in small cubic monoliths (4 cm by side). The mean total porosity was about 15% according to Hg porosimetry measurement (75% of the total porosity being related to pore diameters ≤ 1 μm). An effective diffusion coefficient of 3×10^{-12} m^2/s was fitted by modelling the release profiles of sodium. An identical diffusion coefficient was assigned to all the other elements in a first approximation.

Two batch leaching tests were carried out on finely crushed materials in an airtight device to avoid carbonation. A 48 h liquid/solid contact time was chosen. The first one, the acid neutralization capacity test (ANC), was used to determine lead solubility as a function of pH. The second batch test, related to the maximum mobile fraction (MMF) test, was applied to better characterized the initial chemistry of the waste pore fluids. Typically, batch test have high liquid by solid ratio (L/S = 10 and 50 ml/g here) as well as high reactive surface areas.

Table 1
Reactions and equilibrium constants for minerals used in the calculations

Mineral	Reaction	Log K (25 °C)	Reference
Brucite	$Mg^{2+} + 2\,H_2O \rightarrow Mg(OH)_2 + 2\,H^+$	−16.8	[9]
Calcite	$Ca^{2+} + CO_3^{2-} \rightarrow CaCO_3$	8.5	[9]
CSH 0.8	$0.8\,Ca^{2+} + H_4SiO_4 - 0.4\,H_2O \rightarrow CSH\ 0.8 + 1.6\,H^+$	−11.1	[18, fit]
CSH 1.1	$1.1\,Ca^{2+} + H_4SiO_4 + 0.2\,H_2O \rightarrow CSH\ 1.1 + 2.2\,H^+$	−16.7	[18, fit]
CSH 1.8	$1.8\,Ca^{2+} + H_4SiO_4 + 1.6\,H_2O \rightarrow CSH\ 1.7 + 3.6\,H^+$	−32.6	[18, fit]
Ettringite	$2\,Al^{3+} + 6\,Ca^{2+} + 3\,SO_4^{2-} + 38\,H_2O \rightarrow Ca_6Al_2(SO_4)_3(OH)_{12}{:}26H_2O + 12\,H^+$	−56.9	[19]
Friedel's salt	$4\,Ca^{2+} + 2\,Al^{3+} + 2\,Cl^- + 16\,H_2O \rightarrow Ca_4Al_2Cl_2(OH)_{12}{:}4H_2O + 12\,H^+$	−73.0	[20]
Gibbsite	$Al^{3+} + 3\,H_2O \rightarrow Al(OH)_3 + 3\,H^+$	−8.8	[9]
Gypsum	$Ca^{2+} + SO_4^{2-} + 2\,H_2O \rightarrow CaSO_4{:}2H_2O$	4.9	[9]
Hydrotalcite	$2\,Al^{3+} + 4\,Mg^{2+} + 10\,H_2O \rightarrow Mg_4Al_2O_4(OH)_6 + 14\,H^+$	−73.8	[21]
Portlandite	$Ca^{2+} + 2\,H_2O \rightarrow Ca(OH)_2 + 2\,H^+$	−22.7	[9]
Anglesite	$Pb^{2+} + SO_4^{2-} \rightarrow PbSO_4$	7.8	[9]
Cerussite	$Pb^{2+} + CO_3^{2-} \rightarrow PbCO_3$	13.1	[9]
Hydrocerussite	$3\,Pb^{2+} + 2\,CO_3^{2-} + 2\,H_2O \rightarrow Pb_3(CO_3)_2(OH)_2 + 2\,H^+$	17.5	[9]
Laurionite	$Pb^{2+} + Cl^- + H_2O \rightarrow PbClOH + H^+$	−0.6	[9]
Litharge	$Pb^{2+} + H_2O \rightarrow PbO_2 + 2\,H^+$	−12.7	[9]
$Pb(OH)_2$	$Pb^{2+} + 2\,H_2O \rightarrow Pb(OH)_2 + 2\,H^+$	−11.0	*
$Pb(OH)_3Cl$	$2\,Pb^{2+} + Cl^- + 3\,H_2O \rightarrow Pb(OH)_3Cl + 3\,H^+$	−8.8	[9]

* Adjusted log K from the HATCHES database [10].

Unlike batch tests, the dynamic leaching test used non destructured samples. Consequently, the reactive surface is much lower and more realistic than in batch tests. The global L/S ratio is close to 10. The monolithic waste samples were submitted within a reactor to a permanent renewal flow of the leaching solution; a pure water solution which was regenerated in closed loop by evaporation and recondensation at room temperature. This closed system prevented, or at last minimized, CO_2 uptake. Two flow rates, 5 and 250 ml/h, were applied during two months. In addition, the system was modified to mimic cyclic wetting and drying in open condition with respect to the atmosphere. The cycle was similar to a renewal rate of 250 ml/h. Mineralogical and microstructural studies, performed before and after the tests, relied upon bulk chemical analysis, X-ray diffraction, and scanning electron microscopy (SEM).

3.2. Modelling of pore water and lead solubility

Determining as accurately as possible the initial state (mineralogy and pore water chemistry) of the waste is a prerequisite for applying the model to different experimental or site conditions. The pore water chemistry of S/S waste was indirectly determined from the MMF test and mineralogy [5]. A local equilibrium approach was considered in a first approximation due to high reactive surfaces of the crushed material. Sodium ions were assumed to be both dissolved in pore fluids and sorbed on CSH surfaces, whereas potassium ions were only introduced in pore fluids. The pH was calculated such as to maintain the electroneutrality of the solution which depends itself on the dissolved contents in alkaline ions (present as NaOH and KOH in pore fluids) and portlandite equilibrium. In our model, this last mineral controls the calcium concentration in pore water. Dissolved silica is only controlled by CSH 1.7 whereas sulfate and aluminium are in equilibrium with ettringinte. Chloride was supposed to be present in pore water as well as in a Friedel's salt. The first leaching step is reported in Fig. 1. There is globally a good agreement between modelling and experiment, specially for pH which is a key chemical parameter for pollutant release. The extrapolation of these results leads to a pore water chemistry in the S/S waste enriched in Na–K as major cations and Cl–OH

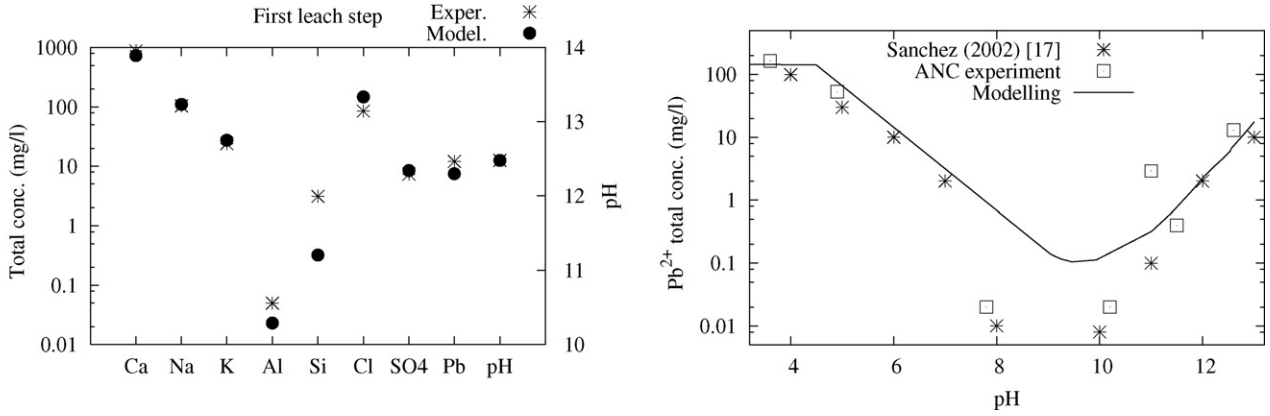

Fig. 1. Evolution of aqueous concentrations and pH during the first step of the sequential MMF test (left) and solubility of lead with pH (closed system) [17].

Table 2
Initial pore water chemistry of the S/S waste and the rain water used in the simulations

Total concentration (mg/l)	S/S waste	Rain water
Na^+	14950	1
K^+	4100	0.2
Ca^{2+}	50	1
Al^{3+}	0.3	–
Pb^{2+}	59	–
H_4SiO_4	100	0.008
Cl^-	5050	1
SO_4^{2-}	1250	1
pH	13.4	6.35

as major anions (see Table 2); pH 13 is related to the alkaline fraction of the pore water.

Fig. 1 reports the dependency of lead solubility with pH in closed condition according to literature, the ANC test and modelling. These results are not essential for estimating the initial pore water chemistry but rather for modelling the release of lead during dynamic leaching tests characterized by a broader range of pH. Noting that the scale is logarithmic, the agreement modelling/experiment is globally satisfactory. The amphoteric behaviour is correctly reproduced, with a solubility minimum found between pH 8 and 10 and a significant increase of solubility in both acidic and alkaline conditions. Modelling indicates that aqueous hydroxide complexes, $Pb(OH)_2$ and $Pb(OH)_3^-$, are the main aqueous species under the alkaline conditions encountered in cement-based waste. Although trace content in oxide and hydroxide are found in cement-based materials, the bulk of lead is incorporated in the matrix of the CSH phases [11]. Sorption processes were not considered here for simplicity and scarcity of sorption mechanistic data. However, globally, lead solubility seems to be controlled by secondary formation of anglesite in the acidic domain, blixite over the range pH 6–10, and lead hydroxide at higher pH. This analysis holds for the test in closed conditions, otherwise (hydro)cerusite controls the solubility over a wide range of pH.

3.3. Modelling of the long-term leaching tests

Modelling was done for the 250 ml/h rate only. To reduce computation time, a cylindrical geometry was used instead of a complete 3D-geometry with a grid size node of 0.15 mm and taking care to minimize errors linked to this cylindrical geometry. Zero-flux conditions were defined at the boundaries of the reactor. No boundary conditions were assigned to the monolithic waste surface. Therefore, pollutant diffusion as well as surface mineralogy can evolve according to the type of circulating fluids.

Fig. 2 shows the evolution of pH over two months in the reactor. Globally, the modelling (250 ml/h only) is in fair agreement with experiment. During the first day, diffusion of the alkaline plume (Na–K–OH) and portlandite dissolution keeps pH at a value of 11 in the reactor. Then, a steady-state comes from the balance between portlandite dissolution and the injection of pure water in the reactor vessel. The higher the rate, the lower the pH in the reactor. In the 250 ml/h case, the pH progressively drops by one unit or more. The cumulative mass releases of Na and Ca for the closed system reactor are also reported in Fig. 2. They are

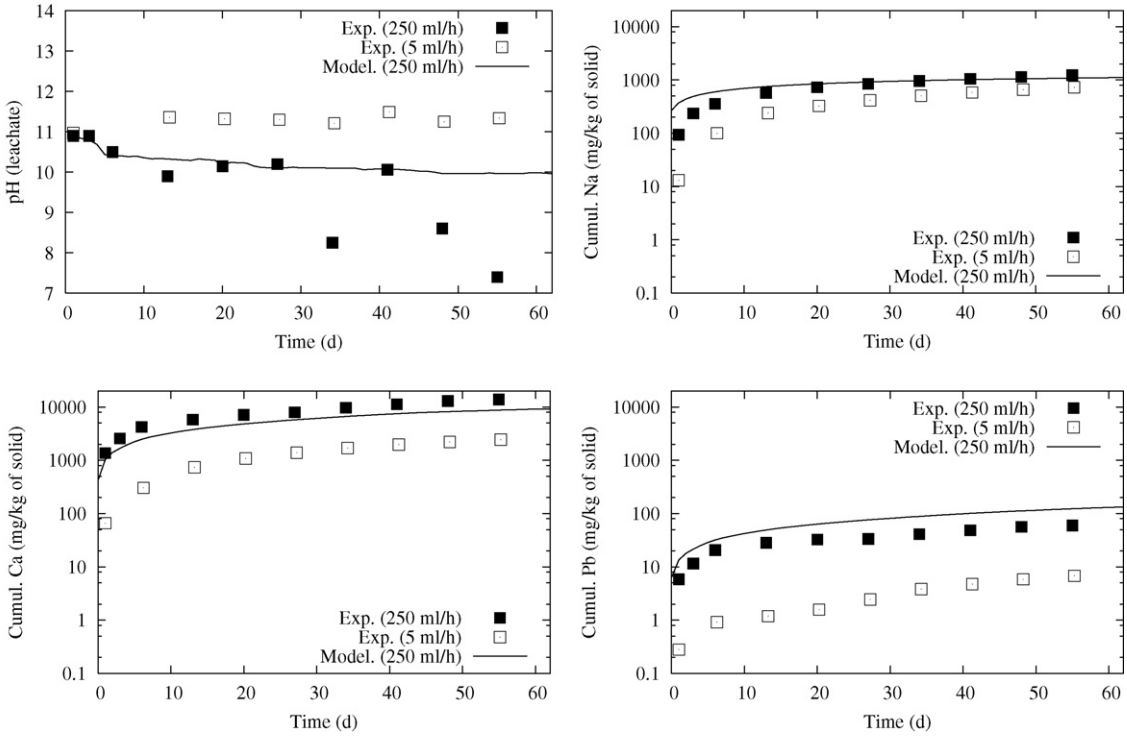

Fig. 2. Evolution of pH and cumulative mass of Na, Ca, Pb (dynamic leaching test in closed conditions).

emblematic of the different leaching behaviours of elements. Na is mainly present in the pore fluid whose stock is progressively exhausted by diffusion, explaining the plateau in the release profile. Ca shows a release dominated by the dissolution of one or several solid phases. Its initial content in the pore fluid is indeed relatively low, and it is the dissolution of portlandite and CSH which feed the leachate, essentially through alteration of the monolithic surface [12,13]. Notwithstanding these contrasted behaviour, there is a good agreement of experimental and modelling results. A good agreement is also achieved for Pb despite the chemical complexity of this element. About 0.5% of the total amount is eventually leached. The calculated mineralogical modifications were restricted to the external surface of the waste monolith with portlandite and CSH 1.7 dissolution and a potential precipitation of CSH of lower Ca/Si ratio. Calcite precipitation was also predicted to continuously occur at the periphery of the monolith under open conditions only, in agreement with SEM observations performed after the dynamic leaching tests.

4. Application to a waste disposal scenario

4.1. Scenario and disposal main features

Hazardous waste repositories are complex engineering facilities. A high level of performance and durability is required by legislation to ensure environmental protection, this demand being usually fulfilled with a multi-barriers approach. The simulation of such systems in all their complexity was out of the scope of the present paper. Our objective was only to illustrate how modelling may be used to extrapolate laboratory results to site conditions. In that respect, the disposal conditions was restricted to a subsystem zoom on the waste and the drainage system assuming a defective cover and therefore rain water infiltration. The simulations consisted in a 2D vertical profile including a micro-disposal (12×6 m) of metric-scale S/S monoliths with a leachate collector at its base (see Fig. 3). The grid node size was 0.1 m. Zero-flux conditions was defined at the boundaries of the collector. No boundary conditions was assigned to the monolithic waste surface.

An average rain water of 740 mm/year was considered, typical of Northern France oceanic climate. One day of the 250 ml/h dynamic leach test roughly corresponds to one equivalent year of rain water infiltration. However, extrapolation of dynamic test to site conditions is far to be straightforward. Among other problems, this strongly depends on the cracking state of the waste as discussed below. The effective infiltration rate of rain water through the defective cover was fixed to 330 mm/year assuming Northern France oceanic climate. This is close to the upper value of Tiruta-Barna et al. [13] for a similar configuration. This is a critical value of the model. A rate ten times lower will roughly lead to a ten times lower release of non or slightly reactive elements. On the other hand, chemical processes, such as carbonation by atmospheric CO_2, are much less sensitive to the infiltration rate. The chemistry of rain water used for the simulation is reported in Table 2. Finally, the partial desaturation state of the monoliths in the waste disposal was not explicitly considered in a first approximation, assuming rain water infiltration in a fully saturated media. However, atmospheric CO_2 penetration within fractures and cracks was partly taken into account in the chemical module.

The chemistry and the mineralogy of the waste monoliths were set exactly identical to those of the small cubic samples used in the dynamic leaching tests. In addition, a very low permeability can be assigned to such undamaged cement-based monoliths [14]. However, ageing and temperature stress under disposal condition may induce a network of connected micro-cracks in the cement-based matrix [7]. Such a network may increase diffusion and leaching [7,12,15]. This process–not taken into account in the laboratory experiments with therefore a possible under-estimation of the long-term environmental impact – was assessed according to a sensitivity analysis. Test-

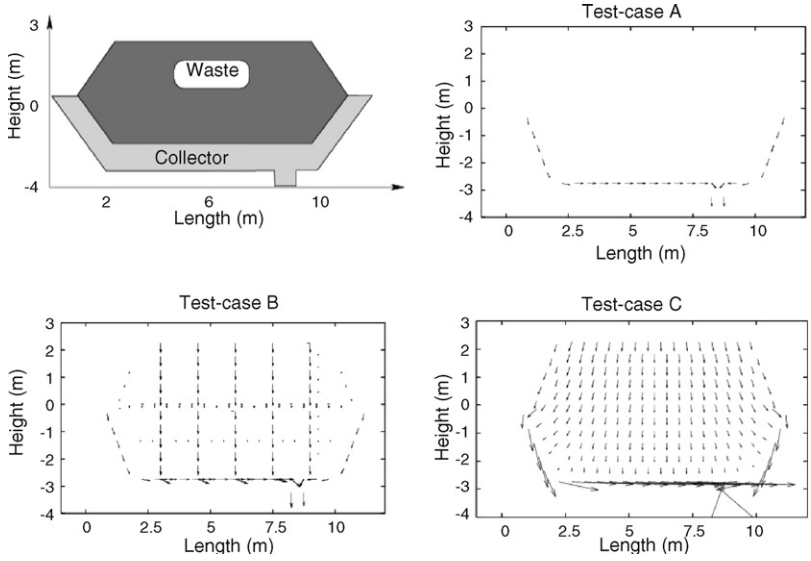

Fig. 3. Darcy flow velocity (units in m/year) in the waste/collector system according to the three monolithe states; test-case C corresponds to flow within the crack-network.

Table 3
Hydrodynamic parameters of the waste disposal for the three test-cases (ω stands for porosity and *De* for effective diffusion coefficient)

	ω (%)	De (m^2/s)	Rain water infiltration
Monolithic waste			
Test-case A = undamaged matrix	15	3×10^{-12}	No infiltration
Test-case B = with fractures[a]	80	8×10^{-10}	Infiltration in the main fractures only
Test-case C = block-matrix[b]	15	3×10^{-12}	Infiltration within the crack-network over the whole upper waste surface
Cracks[c]	2	2×10^{-11}	
Collector	100	1×10^{-9}	

[a] Parameters for the fractures only, the matrix parameters are identical to test-case A.
[b] 10 cm by side *L*.
[c] 2% porosity corresponds to an average fracture width of 2 mm.

case A considered undamaged monoliths without any cracks (see Table 3). In test-case B, monoliths showed an undamaged matrix but presented some transversal, and more or less connected, multi-centimetric fractures. At last, test-case C assumed monoliths with a dense network of micro-cracks. Such cracks in cement-based materials generally interconnect flow path and increase permeability by many orders of magnitude [16]. The physical containment of the disposal system decreases from test-cases A to C.

4.2. Long-term disposal evolution and pollutant fates

The HYTEC code was used to simulate – in a coupled way – flow and transport through the system, the initial chemistry and mineralogy of S/S waste and their evolution, and the cumulative release of elements in the leachate collector. Fig. 3 exhibits the Darcy flow velocities calculated for the different test-cases. Without micro-cracks, the monoliths are an efficient physical barrier against infiltration. The equivalent L/S ratio is almost nil corresponding to the pore water on solid mass ratio only. The occurrence of transversal fractures results in a channelized circulation within the waste zone and increase moderately the rate at the collector basement. The L/S increases locally in the fracture environment but remains globally low. Infiltration is, on the contrary, significantly emphasized if rain water can percolate from the entire waste surface into the crack-networks, as pessimistically assumed in the dual porosity calculation of test-case C. The L/S increases too but moderately. However, comparatively, the reactive surface area increases much more when the monoliths are subdivided in block-matrix of 10 cm by side *L*.

Fig. 4 gives a typical example of system evolution modelling, with pH and aqueous lead profiles calculated after 100 years for all test-cases. The analysis of test-case B is the most informative due to its intermediate behaviour between test-cases A and C.

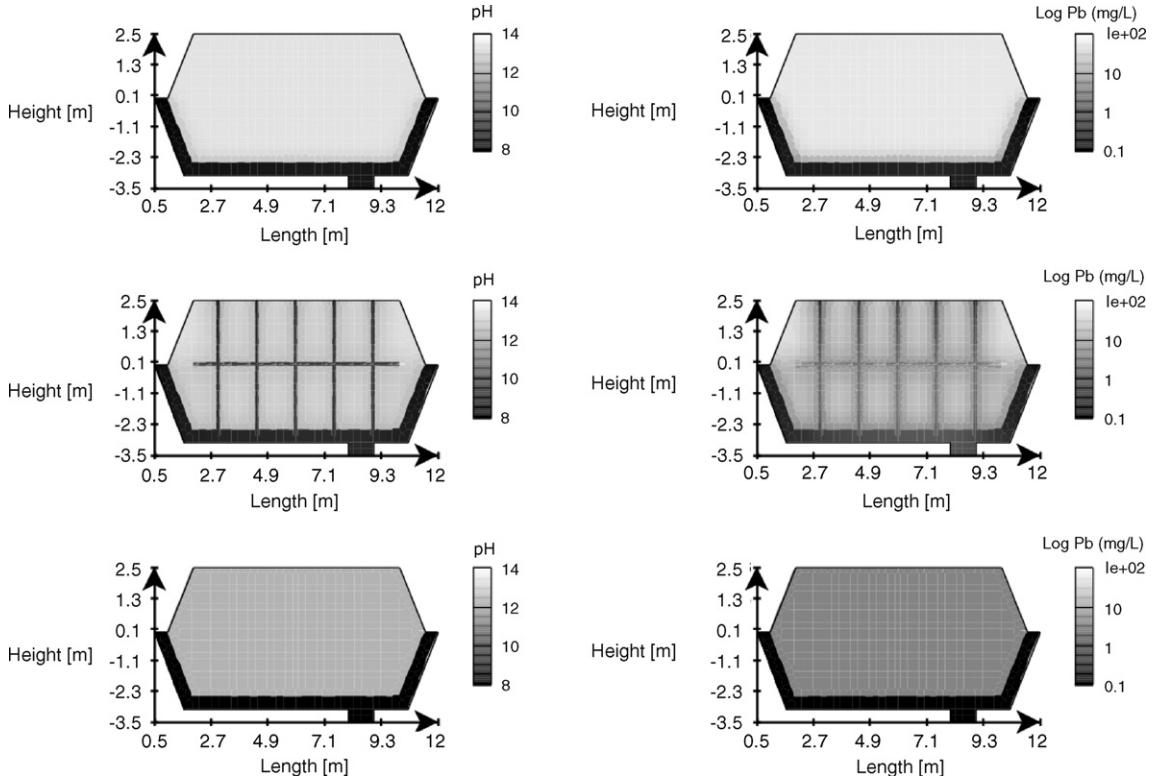

Fig. 4. Calculated pH and lead solubility after 100 years for test-case A (top), B (middle) and C (bottom); test-case C corresponds to the block-matrix.

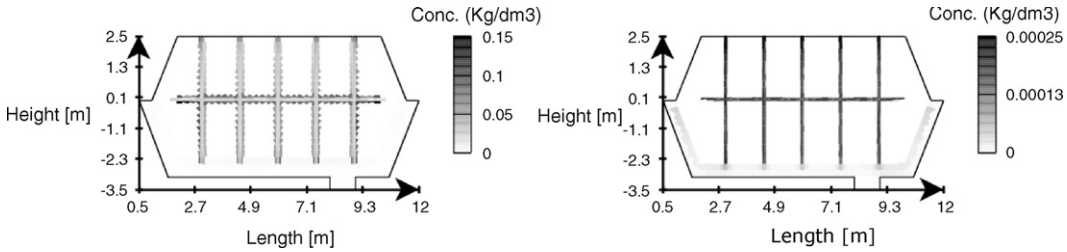

Fig. 5. Precipitation of calcite (left) and cerussite (right) after 100 years for test-case B.

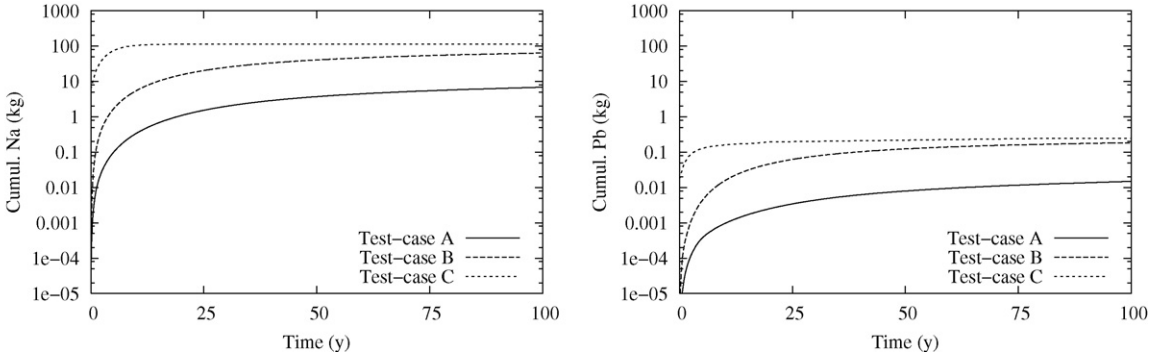

Fig. 6. Na and Pb cumulative masses calculated at the collector base for all the test-cases.

In test-case B, the pH slowly decreases in the monolith matrix owing to the diffusion of alkaline ions in the main fractures and their subsequent advective transport to the collector bottom. The huge quantity of portlandite buffers on the long term the pH around 12.3, as in the MMF batch tests. This is the overall process. However, pH is lower in the fracture environment due to water infiltration but, above all, CO_2 penetration. CO_2 reacts with portlandite yielding calcite precipitation (carbonation) in the surrounding matrix, as shown in Fig. 5. Calcite precipitation and lowering of pH are commonly observed in experiments, like for instance in the present dynamic leach test performed in open-conditions. The potential sealing effect at the fracture walls induced by calcite precipitation was not considered in the calculations. Lead diffusion from the matrix induces cerussite precipitation in the fracture (Fig. 5). By comparison, test-case A shows neither significant pH evolution nor calcite precipitation. Lead solubility remains therefore high in such strongly alkaline pore water but, at the same time, cannot migrate outside the waste. In test-case C, the alkaline ions are quickly leached away and lead solubility drops as pH decreases. Calcite precipitation occurs preferentially at the bottom of the waste zone. Again, sealing or self-healing of micro-cracks raises the possibility of sealing effect and, consequently, hindrance of pollutant release.

Fig. 6 gives the calculated cumulative mass releases of Na and Pb collected in the drainage system according to the three test-cases. As indicated by the dynamic leach tests, Na can be assimilated to a tracer in cement-base waste. This cation is thus a relevant quantitative indicator of the effect of the hydrodynamic regime on chemical species release. The generalized cracking state leads to a full exhaustion of the Na stock after a few dozen years. By comparison, the complete release of Na in the dynamic leach test takes about one month in agreement with smaller block size (4 cm compared to 10 cm in test-case C). To the opposite, in the case of undamaged waste, the release is efficiently restrained and restricted to those monoliths located at the waste bottom. The transversal fractures permit an internal but partial drainage of the waste zone and leads to intermediate results between test-cases A and C. With regard to lead, damaged monoliths can, at the extreme, release one-hundred times more masses than undamaged S/S waste. However, even in test-case C, less than 0.1% of the total Pb waste inventory is released ultimately. Indeed, if the hydrodynamics of test-case C clearly favors lead mobility, at the same time this configuration leads to a quicker pH drop and therefore a sharper decrease of lead solubility in the matrix. The mobility of lead in the overall system, fracture and matrix, is a combination of both aqueous chemistry and hydrodynamics.

5. Conclusions

The studied S/S cement-based waste was characterized by minimal mass-transfers due to weak values of porosity, diffusion coefficient and permeability, at least in the absence of connected micro-cracks. A reactive transport model was used to assess its long-term behaviour in the scope of waste disposal or even recycling. The model was based on batch and dynamic leaching tests as well as mineralogical investigations. Coupling between hydrodynamic and chemical processes was required to simulate the complexity of waste evolution and pollutant fate in both the dynamic leach tests and the disposal scenario. Despite the chemical complexity of cement-based waste, the capability of a single and consistent model to simulate – to some levels of accuracy – a variety of experimental conditions (batch or dynamic test) and flow patterns brings confidence in its application to long-term, large-scale site conditions. Furthermore, this methodological

approach is enforced by the technical possibilities of reactive transport codes to deal with realistic geometries, boundary conditions and hydrodynamic regimes. With this respect, it should be noted that the waste disposal configuration and scenario were clearly simplified. In particular, the effect of the crack-network was exaggerated for the purpose of reactive transport illustration. Further studies are in progress, taking into better account unsaturated conditions, carbonation effect and, more technically, the role of clay liners.

Acknowledgments

The editorial handling of Professor A. Nzihou as well as constructive comments of two anonymous reviewers are gratefully acknowledged.

References

[1] P. Moszkowicz, F. Sanchez, R. Barna, J. Méhu, Pollutants leaching behaviour from solidified wastes: a selection of adapted various models, Talanta 46 (1998) 375–383.
[2] P. Baranger, M. Azaroual, P. Freyssinet, S. Lanini, P. Piantone, Weathering of a MSW bottom ash heap: a modelling approach, Waste Manage. 22 (2002) 173–179.
[3] L. Tiruta-Barna, A. Imyim, R. Barna, Long-term prediction of the leaching behavior of pollutants from solidified wastes, Adv. Environ. Res. 8 (2004) 697–711.
[4] J. van der Lee, L. De Windt, Present state and future directions of modeling geochemistry in hydrogeological systems, J. Contam. Hydrol. 47 (2001) 265–282.
[5] L. De Windt, R. Badreddine, Modelling of long-term dynamic leaching tests applied to solidified/stabilized waste, Waste Manage., to be published.
[6] M. Atkins, F.P. Glasser, Application of Portland cement-based materials to radioactive waste immobilization, Waste Manage. 12 (1992) 105–131.
[7] J. Yvon, D. Antenucci, E. Jdid, G. Lorenzi, V. Dutre, D. Leclerq, P. Nielsen, M. Veschkens, Long-term stability in landfills of municipal solid waste incineration fly ashes solidified/stabilized by hydraulic binders, J. Geochem. Explor., (2006) in press.
[8] J. van der Lee, L. De Windt, V. Lagneau, P. Goblet, Module-oriented modeling of reactive transport with HYTEC, Comput. Geosci. 29 (2003) 265–275.
[9] J.D. Allison, D.S. Brown, K.J. Novo-Gradac, MINTEQA2/PRODEF2, A Geochemical Assessment Model for Environmental Systems: Version 3.0 User's Manual, EPA/600/3-91/021, U.S. EPA, Athens, GA 30605, 1991.
[10] Hatches. Hatches-r10, database for radio chemical modelling. Technical report, NEA, 1991.
[11] R. Badreddine, A.-N. Humez, U. Mingelgrin, A. Benchara, F. Meducin, R. Prost, Retention of trace metals by solidified/stabilized wastes: assessment of long-term metal release, Environ. Sci. Technol. 38 (2004) 1383–1398.
[12] M. Andac, F.P. Glasser, Long-term leaching mechanisms of Portland cement-stabilized municipal solid waste fly ash in carbonated water, Cement Concrete Res. 29 (1999) 179–186.
[13] L. Tiruta-Barna, Z. Rethy, R. Barna, Release dynamic process identification for a cement based material in various leaching conditions. Part II. Modelling the release dynamics for different leaching conditions, J. Environ. Manage. 74 (2005) 127–139.
[14] W.J. McCarter, G. Starrs, T.M. Chrisp, Electrical conductivity, diffusion, and permeability of Portland cement-based mortars, Cement Concrete Res. 30 (2000) 1395–1400.
[15] G. Tognazzi, J.M. Torrenti, M. Carcasses, J.P. Ollivier, Coupling between diffusivity and cracks in cement-based systems, Mater. Res. Soc. Proc. 608 (2000) 325–330.
[16] K. Wang, D.C. Jansen, S.P. Shah, Permeability study of cracked concrete, Cement Concrete Res. 27 (3) (1997) 381–393.
[17] F. Sanchez, C. Gervais, A.C. Garrabrants, R. Barna, D.S. Kosson, Leaching of inorganic contaminants from cement-based waste materials as a result of carbonation during intermittent wetting, Waste Manage. 22 (2002) 249–260.
[18] S.A. Stronach, F.P. Glasser, Modeling the impact of abundant geochemical components on phase stability and solubility of the $CaO–SiO_2–H_2O$ systems at 25 °C: Na^+, K^+, SO_4^{2-}, Cl^- and CO_3^{2-}, Adv. Cement Res. 9 (1997) 167–181.
[19] R.B. Perkins, C.D. Palmer, Solubility of ettringite ($Ca_6[Al(OH)_6]_2(SO_4)_3{\cdot}26H_2O$) at 5–75 °C, Geochim. Cosmochim. Acta 63 (1999) 1969–1980.
[20] J.V. Bothe Jr., P.W. Brown, PhreeqC modeling of Friedel's salt equilibria at 23 °C, Cement Concrete Res. 34 (2004) 1057–1063.
[21] D.G. Bennet, D. Read, M. Atkins, F.P. Glasser, A thermodynamic model for blended cements. II: Cement hydrate phases, thermodynamic values and modelling studies, J. Nucl. Mater. 190 (1992) 315–325.